Fluorescent Probes

International Edition: DOI: 10.1002/anie.201603328
German Edition: DOI: 10.1002/ange.201603328

Detection of *LacZ*-Positive Cells in Living Tissue with Single-Cell Resolution

Tomohiro Doura, Mako Kamiya, Fumiaki Obata, Yoshifumi Yamaguchi, Takeshi Y. Hiyama, Takashi Matsuda, Akiyoshi Fukamizu, Masaharu Noda, Masayuki Miura, and Yasuteru Urano**

Abstract: *The LacZ gene, which encodes Escherichia coli β-galactosidase, is widely used as a marker for cells with targeted gene expression or disruption. However, it has been difficult to detect lacZ-positive cells in living organisms or tissues at single-cell resolution, limiting the utility of existing lacZ reporters. Herein we present a newly developed fluorogenic β-galactosidase substrate suitable for labeling live cells in culture, as well as in living tissues. This precisely functionalized fluorescent probe exhibited dramatic activation of fluorescence upon reaction with the enzyme, remained inside cells by anchoring itself to intracellular proteins, and provided single-cell resolution. Neurons labeled with this probe preserved spontaneous firing, which was enhanced by application of ligands of receptors expressed in the cells, suggesting that this probe would be applicable to investigate functions of targeted cells in living tissues and organisms.*

Analysis at the single-cell level is increasingly important for understanding the heterogeneity of cell populations and for defining specific cell types or cell states in complex networks in animals and plants, or their tissues.[1–3] *LacZ* reporter which encodes *Escherichia coli* β-galactosidase is a powerful reporter in combination with synthetic substrates,[4] and numerous *lacZ* reporter animals have been established to detect a target subpopulation of cells, to examine transcriptional regulation, or to evaluate targeted gene expression or disruption. Since substrates for β-galactosidase can be activatable (chromogenic or fluorogenic), the sensitive and rapid detection of *lacZ*(+) cells is feasible in principle without the need to wash out unreacted/unbound substrates. But unfortunately, X-Gal, a commonly used chromogenic substrate,[5] is only applicable to fixed cells or tissues, making it difficult to label and track selected cell populations or to examine cellular responses of targeted cells in living samples. Fluorogenic substrates for visualizing β-galactosidase activity in living cells have been extensively developed, but so far, selective labeling of *lacZ*(+) cells with single-cell resolution in living tissues has not been reported. Therefore, a new generation of fluorogenic substrates capable of selective imaging of *lacZ*(+) cells in living samples with single-cell resolution is needed.

Herein, we describe a new class of functionalized fluorogenic substrates for β-galactosidase, suitable for selective imaging of *lacZ*(+) cells in living samples. For this purpose, we focused on modifying our previously reported fluorogenic substrates for β-galactosidase, HMDER-βGals,[6,7] whose fluorescence is controlled by utilizing intramolecular spirocyclization. HMDER-βGal has sufficient cell permeability to visualize β-galactosidase activity in living tissue, but its fluorescent hydrolysis product, HMDER, tends to leak out of cells during prolonged incubation. Thus, to retain the fluorescent product inside cells, we set out to integrate quinine methide chemistry into our design strategy. Quinone methide chemistry is widely used in the design of enzyme inhibitors,[8] activity-based probes,[9] self-immobilizing fluorogenic substrates,[10,11] prodrugs,[12] and for chemical selection of catalytic antibodies.[13,14] Therefore, we incorporated a leaving group at the 4th position of HMDER-βGal, so that the enzymatic reaction would produce a quinone methide intermediate (Figure 1, Figure S1 in the Supporting Information). We selected a fluoromethyl or difluoromethyl leaving group, and newly prepared two derivatives, designated as Spiro-based immobilisable diethylrhodol-βGal-1 and -2 (SPiDER-βGal-1 and -2), respectively (Figure 1).

To confirm that our design strategy works, we evaluated the photophysical properties of the SPiDER-βGals in aque-

[*] Dr. T. Doura, Dr. M. Kamiya, Prof. Y. Urano
Graduate School of Medicine
The University of Tokyo
7-3-1, Hongo, Bunkyo-ku, Tokyo 113-0033 (Japan)
E-mail: mkamiya@m.u-tokyo.ac.jp
uranokun@m.u-tokyo.ac.jp
Dr. F. Obata, Dr. Y. Yamaguchi, Prof. M. Miura, Prof. Y. Urano
Graduate School of Pharmaceutical Sciences, The University of Tokyo
7-3-1 Hongo, Bunkyo-ku, Tokyo, 113-0033 (Japan)
Dr. M. Kamiya, Dr. Y. Yamaguchi
PRESTO, Japan, Science and Technology Agency
4-1-8 Honcho, Kawaguchi, Saitama, 332-0012 (Japan)
Dr. T. Y. Hiyama, Prof. M. Noda
Division of Molecular Neurobiology, National Institute for Basic Biology
5-1 Higashiyama, Myodaiji-cho, Okazaki, Aichi, 444-8787 (Japan)
Dr. T. Y. Hiyama, T. Matsuda, Prof. M. Noda
School of Life Science, The Graduate University for Advanced Studies
5-1 Higashiyama, Myodaiji-cho, Okazaki, Aichi, 444-8787 (Japan)
Prof. A. Fukamizu
Life Science Center, Tsukuba Advanced Research Alliance
Tsukuba, Ibaraki, 305-8577 (Japan)
and
Graduate School of Life and Environmental Sciences, University of Tsukuba
Tsukuba, Ibaraki, 305–8577 (Japan)
Prof. M. Miura, Prof. Y. Urano
CREST, Japan, Agency for Medical Research and Development
1-7-1 Otemachi, Chiyoda-ku, Tokyo, 100-0004 (Japan)

Supporting information for this article can be found under: http://dx.doi.org/10.1002/anie.201603328.

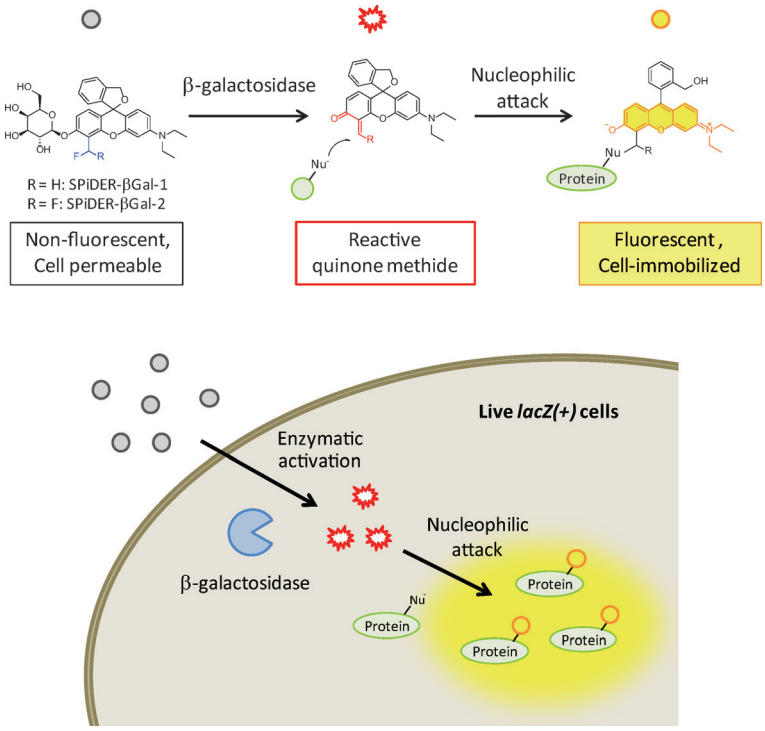

Figure 1. Functionalized fluorogenic substrates for β-galactosidase (SPiDER-βGals). When the β-galactoside moiety is cleaved by the enzyme, activation of fluorescence and activation of binding ability to intracellular proteins occur simultaneously, so that the fluorescent product is immobilized in living cells.

ous solution, compared with parental HMDER-βGal. Introduction of the leaving groups caused little shift in absorption or emission wavelength, though pK_{cycl} was reduced (i.e., the pH value at which the extent of spirocyclization is sufficient to reduce the absorbance of the compound to one-half of the maximum absorbance; Table 1, Figures S1,S2). Density functional theory (DFT) calculations indicated that introduction of a fluoromethyl or difluoromethyl group decreases the lowest unoccupied molecular orbital (LUMO) energy level of the fluorophores, suggesting that the spirocyclic form is more stabilized than in the original form (Table S1). As expected, SPiDER-βGals predominantly exist in colorless, non-fluorescent spirocyclic form at physiological pH of 7.4, but are converted into colored and fluorescent hydrolysis products upon reaction with the enzyme, showing a drastic increase in fluorescence intensity (Figures S3,S4). SPiDER-βGal-1 and SPiDER-βGal-2 showed similar enzyme reactivity and kinetics in vitro (Figure S5). However, importantly, SPiDER-βGal-1 shows greater fluorescence activation both in the absence and presence of proteins such as bovine serum albumin (BSA; 650-fold and 990-fold increase, respectively) than SPiDER-βGal-2 (210-fold and 70-fold increase, respectively; Figures S3,S6).

Table 1: Photochemical Properties of SPiDER-βGals, HMDER-βGal, and the enzyme-catalyzed hydrolysis products.

Compound	Absorption maximum/ nm	Emission maximum/ nm	Φ_{fl}	pK_{cycl}	pK_a	Activation ratio
SPiDER-βGal-1	493, 525	560	<0.01[a]	6.3	–	>650-fold
SPiDER-βGal-2	493, 525	560	<0.01[a]	6.0	–	>210-fold
HMDER-βGal	493, 525	536	0.009[d]	6.9	–	>70-fold
4-CH_2OH HMDER	526	553	0.13[b]	11.4	4.9	–
4-CHO HMDER	524	556	0.08[c]	10.4	3.9	–
HMDER	525	543	0.14[d]	11.3	5.4	–

[a] Measured in 200 mM sodium phosphate buffer, pH 2.0, containing 0.1% DMSO as a cosolvent. [b] Measured in 200 mM sodium phosphate buffer, pH 7.4, containing 0.07% DMSO as a cosolvent. [c] Measured in 200 mM sodium phosphate buffer, pH 7.4, containing 0.5% DMSO as a cosolvent. [d] Reference [6].

We examined the binding ability of SPiDER-βGals upon enzymatic activation in HEK-*lacZ*(+) cells by analyzing the cell lysates by SDS-PAGE. Fluorescence was ubiquitously observed throughout the mass range of proteins after treatment with SPiDER-βGals, but not with HMDER-βGal, indicating that activated SPiDER-βGals randomly bound to intracellular proteins.[15] Substantial fluorescence was also observed at the electrophoretic leading edge, where activated probes may have been trapped by small-molecular nucleophiles, such as free amino acids, glutathione, and water (Figure 2a). SPiDER-βGal-1 shows superior labeling efficiency to the intracellular components compared with SPiDER-βGal-2. This result is in accordance with the previous reports that difluoromethyl phenol is more stable than its monofluoro analogue.[16] These results demonstrate the suitability of SPiDER-βGal-1 for our purpose, so we focused on SPiDER-βGal-1 for further evaluation in living cells and tissues.

We also confirmed that SPiDER-βGal-1 is superior to commercially available probes (HMDER-βGal and C_{12}FDG) in terms of cellular permeability and retention, since only the fluorescent product of SPiDER-βGal-1 was well retained in the cells after washing out or fixation of cells (Figure 2b, Figure S7). These results supported the effectiveness of our strategy of immobilizing SPiDER-βGal-1 on cellular components after activation in *lacZ*(+) cells. We next applied the probes to a co-culture of HEK-*lacZ*(+) cells and HEK-*lacZ*(−) cells. Indeed, SPiDER-βGal-1 enabled us to distinguish these cells with high signal-to-noise (S/N) ratio at single-cell resolution, whereas HMDER-βGal stained both types of cells due to diffusion of HMDER (Figure 2c). The S/N ratio obtained with SPiDER-βGal-1 was sufficient for discrimination of *lacZ*(+) cells and *lacZ*(−) cells by flow cytometry (Figure 2d), which has not been achieved with commercially available or reported probes under such mild conditions. However, labeling conditions need to be optimized, since SPiDER-βGal-1 might exhibit cytotoxicity depending on factors such as applied dye concentration, incubation time, cell type, and *lacZ* expression level (Figure S8).

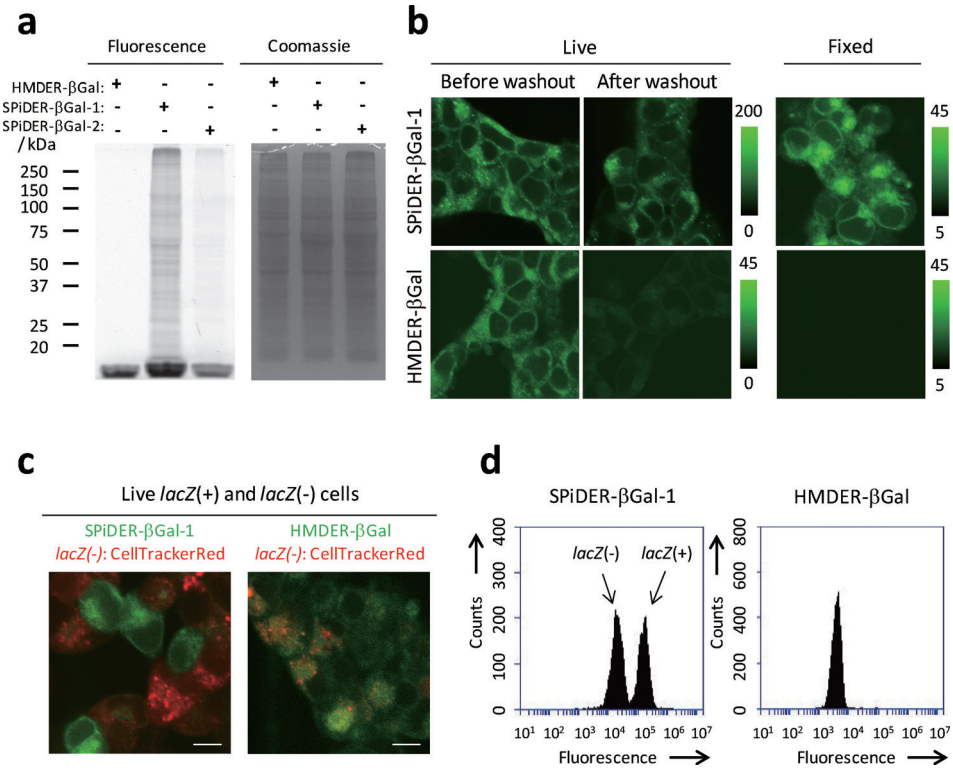

Figure 2. *LacZ*(+) cell-selective live imaging with SPiDER-βGal-1. a) SDS-PAGE analyses of lysate of HEK-*lacZ*(+) cells pre-treated with SPiDER-βGal-1, SPiDER-βGal-2, or HMDER-βGal. b) Fluorescence images of HEK-*lacZ*(+) cells treated with 1 μM SPiDER-βGal-1 or HMDER-βGal for 1 h (left), followed by washout (middle), and fixation with 4% paraformaldehyde (PFA) (right). Ex/Em = 525 nm/535–595 nm. Scale bars, 10 μm. c) Live imaging of HEK-*lacZ*(+) cells and HEK-*lacZ*(−) cells with SPiDER-βGal-1 or HMDER-βGal. HEK-*lacZ*(−) cells were pre-stained with CellTracker Red. Scale bars, 10 μm. d) Flow cytometric analyses of a mixture of HEK-*lacZ*(+) cells and HEK-*lacZ*(−) cells pre-treated with SPiDER-βGal-1 or HMDER-βGal.

To confirm the applicability of SPiDER-βGal-1 for *lacZ* reporters in other model organisms, we performed ex vivo imaging of cultured tissues of *Drosophila melanogaster*. We first tried fluorescence imaging of live larval wing discs, a precursor structure of a part of the adult thorax including the wing. Simple incubation with SPiDER-βGal-1 for 30 min visualized *lacZ*(+) cells in the tissue with a clear borderline between *lacZ*(+) and *lacZ*(−) regions (Figure 3a, Figures S9,S10, Movies S1 and S2). Optical sectioning with a confocal laser microscope revealed the three-dimensional spatial pattern of *lacZ* expression with single-cell resolution (Movie S3), which is not achievable with conventional X-Gal staining. We also applied SPiDER-βGal-1 to flip-out clones in larval fat body, in which β-galactosidase is expressed stochastically in cells with scattered distribution. Single *lacZ*(+) cells in the live fat body could be clearly visualized within a few minutes (Figure 3b, Figure S11, Movie S4), and optical sectioning afforded dual-color three-dimensional images (Movie S5). As observed in the cultured cells, the fluorescence staining was resistant to fixation, and *lacZ*(+) cells in prefixed tissue can also be visualized (Figure S12). We confirmed the fluorescence signal produced by SPiDER-βGal-1 was co-localized with *anti*-βGal immunostaining, demonstrating that *lacZ* is expressed in cells fluorescently labeled with SPiDER-βGal-1 (Figure 3b, Movie S6). SPiDER-βGal-1 also visualized single β-galactosidase-expressing intestinal stem cells or enteroblasts in live and fixed *Drosophila* midgut (Figure S13, Movie S7).

We investigated whether SPiDER-βGal-1 is applicable to detect *lacZ*(+) cells in mammalian living tissues. We first carried out ex vivo imaging of live mouse tissues freshly collected from $Cp2l1^{+/lacZ}$ mice.[17] After 30 min incubation with SPiDER-βGal-1, we could visualize *lacZ*(+) cells in the duct of salivary gland and in renal tubule cells of kidney (Figures S14,S15).[18] Next, we tested whether the SPiDER-βGal-1-labelled cells retain their physiological function by means of electrophysiological analysis. Acute coronal brain slices obtained from $AT1a^{+/lacZ}$ mice, in which β-galactosidase is expressed in angiotensin II type 1A receptor (AT1a)-positive neurons,[18] were incubated with SPiDER-βGal-1 for 15 min at room temperature. Fluorescence signals were observed in paraventricular nucleus (PVN), where AT1a expression has been reported (Figures S16,S17).[19] We confirmed that SPiDER-βGal-1 signals in the PVN were specifically localized to β-galactosidase-positive cells by immunostaining (Figure 3c). To test the compatibility of SPiDER-βGal-1 labeling with electrophysiological analysis, the firing activity of the cells was examined with a patch clamp method (Figure 3d). We selected weakly stained neurons in which cellular functions are likely to be better maintained. The cells showed spontaneous firing activities under the basal condition, and continuous application of angiotensin II (2 μM) resulted in an enhancement of the spike frequency. The frequency of the firing activity was comparable to that previously reported in rat.[20] These results indicate that the SPiDER-βGal-1-labeled neurons were still alive and retained subcellular signaling mechanisms downstream of angiotensin II receptor. This result demonstrated that SPiDER-βGal-1 can specifically visualize target *lacZ*(+) neurons even in the complex network of the brain, and is compatible with electrophysiological analysis.

By integrating quinine methide chemistry with control of fluorescence by intramolecular spirocyclization, we have designed SPiDER-βGal-1 as a novel probe for β-galactosidase activity; the enzyme simultaneously activates both fluorescence and binding ability to intracellular proteins in living cells. This probe enabled selective and rapid detection

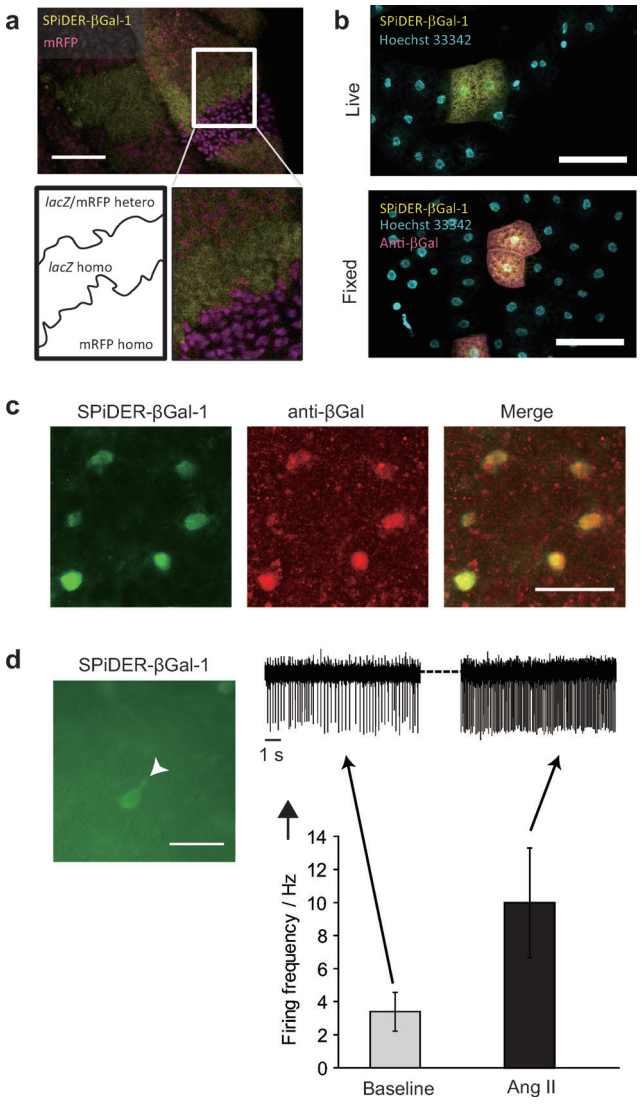

Figure 3. Ex vivo imaging of *Drosophila melanogaster* and mice tissue. a) Live staining of complementary genetic mosaic clones in wing discs by using SPiDER-βGal-1. Three different staining patterns were observed, corresponding to the three genotypes; homozygous for *arm-lacZ*, homozygous for *His2Av-mRFP1*, and heterozygous for both genotypes. Scale bar, 40 μm. b) Fluorescent staining of *lacZ*(+) flip-out clones in live and fixed larval fat body; nuclear co-staining with Hoechst 33342 (blue). Immunohistochemical staining of β-galactosidase was performed after fixation (pink) for the lower panel. Scale bars, 100 μm. c) Double staining of brain sections obtained from *AT1a*$^{+/lacZ}$ mice using SPiDER-βGal-1 and *anti*-β-galactosidase antibody. Acute brain sections were stained with SPiDER-βGal-1, and then fixed and used for immunohistochemical staining with *anti*-β-galactosidase antibody. Scale bar, 50 μm. d) Electrophysiological recordings from neurons labeled with SPiDER-βGal-1. Left: representative SPiDER-βGal-1-labelled neuron in the PVN (arrowheads). Scale bar, 50 μm. Right: spike frequency of neurons labeled with SPiDER-βGal-1. The firing activity of neurons was enhanced by application of 2 μM angiotensin II. Representative traces of the loose-patch recordings are shown in the upper insets. Data are mean ± SD ($n = 5$).

of live *lacZ*(+) cells at single-cell resolution without perturbing cellular functions; not only can three-dimensional morphological information about the target cells and surrounding tissues be obtained with the aid of confocal microscopy, but also the firing activities of targeted neurons in living brain slices can be monitored by electrophysiological analysis. Considering the large available stock of *lacZ* reporter mouse lines, this probe should drastically expand the utility of *lacZ* reporters, serving as a truly indispensable tool for investigating the functions/fate of individual cells in living tissues and animals, with the potential to provide unprecedented insights.

Acknowledgements

This research was supported in part by the Ministry of Education, Culture, Sports, Science and Technology of Japan (Grant-in-Aid for Scientific Research (KAKENHI), grants 26111012 and 16H02606 to Y.U., grant 15H05951 to M.K., grants 26111726 and 26293043 to T.Y.H., grants by the Brain Mapping by Integrated Neurotechnologies for Disease Studies (Brain/MINDS) to Y.U.), by JSPS Core-to-Core Program, A. Advanced Research Networks (to Y.U.), by The Daiichi-Sankyo Foundation of Life Science (grant to Y.U.), by Japan foundation for applied enzymology (to M.K.). We thank Dr. Kazunari Hisadome for helpful discussions.

Keywords: fluorescent probes · *lacZ* · quinone methide intermediates · single-cell resolution · β-galactosidase

How to cite: *Angew. Chem. Int. Ed.* **2016**, *55*, 9620–9624
Angew. Chem. **2016**, *128*, 9772–9776

[1] Q. Deng, D. Ramsköld, B. Reinius, R. Sandberg, *Science* **2014**, *343*, 193–196.
[2] F. Tang, K. Lao, M. A. Surani, *Nat. Methods* **2011**, *8*, S56–59.
[3] A. J. Hughes, D. P. Spelke, Z. Xu, C.-C. Kang, D. V. Schaffer, A. E. Herr, *Nat. Methods* **2014**, *11*, 749–755.
[4] D. J. Spergel, U. Krüth, D. R. Shimshek, R. Sprengel, P. H. Seeburg, *Prog. Neurobiol.* **2001**, *63*, 673–686.
[5] K.-L. Laugwitz, A. Moretti, J. Lam, P. Gruber, Y. Chen, S. Woodard, L.-Z. Lin, C.-L. Cai, M.-M. Lu, M. Reth, O. Platoshyn, J. X.-J. Yuan, S. Evans, K. R. Chien, *Nature* **2005**, *433*, 647–653.
[6] M. Kamiya, D. Asanuma, E. Kuranaga, A. Takeishi, M. Sakabe, M. Miura, T. Nagano, Y. Urano, *J. Am. Chem. Soc.* **2011**, *133*, 12960–12963.
[7] D. Asanuma, M. Sakabe, M. Kamiya, K. Yamamoto, J. Hiratake, M. Ogawa, N. Kosaka, P. L. Choyke, T. Nagano, H. Kobayashi, Y. Urano, *Nat. Commun.* **2015**, *6*, 6463.
[8] J. Myers, T. Widlanski, *Science* **1993**, *262*, 1451–1453.
[9] C.-P. Lu, C.-T. Ren, S.-H. Wu, C.-Y. Chu, L.-C. Lo, *ChemBioChem* **2007**, *8*, 2187–2190.
[10] T. Komatsu, K. Kikuchi, H. Takakusa, K. Hanaoka, T. Ueno, M. Kamiya, Y. Urano, T. Nagano, *J. Am. Chem. Soc.* **2006**, *128*, 15946–15947.
[11] D. H. Kwan, H.-M. Chen, K. Ratananikom, S. M. Hancock, Y. Watanabe, P. T. Kongsaeree, A. L. Samuels, S. G. Withers, *Angew. Chem. Int. Ed.* **2011**, *50*, 300–303; *Angew. Chem.* **2011**, *123*, 314–317.
[12] K. Haba, M. Popkov, M. Shamis, R. A. Lerner, C. F. Barbas, D. Shabat, *Angew. Chem. Int. Ed.* **2005**, *44*, 716–720; *Angew. Chem.* **2005**, *117*, 726–730.
[13] K. D. Janda, L.-C. Lo, C.-H. L. Lo, M.-M. Sim, R. Wang, C.-H. Wong, R. A. Lerner, *Science* **1997**, *275*, 945–948.

[14] S. Cesaro-Tadic, D. Lagos, A. Honegger, J. H. Rickard, L. J. Partridge, G. M. Blackburn, A. Plückthun, *Nat. Biotechnol.* **2003**, *21*, 679 – 685.
[15] J. L. Bolton, S. B. Turnipseed, J. A. Thompson, *Chem.-Biol. Interact.* **1997**, *107*, 185 – 200.
[16] V. Ahmed, Y. Liu, S. D. Taylor, *ChemBioChem* **2009**, *10*, 1457 – 1461.
[17] Y. Yamaguchi, S. Yonemura, S. Takada, *Development* **2006**, *133*, 4737 – 4748.
[18] T. Sugaya, S. Nishimatsu, K. Tanimoto, E. Takimoto, T. Yamagishi, K. Imamura, S. Goto, K. Imaizumi, Y. Hisada, A. Otsuka, H. Uchida, M. Sugiura, K. Fukuta, A. Fukamizu, K. Murakami, *J. Biol. Chem.* **1995**, *270*, 18719 – 18722.
[19] C. Premer, C. Lamondin, A. Mitzey, R. C. Speth, M. S. Brownfield, *Int. J. Hypertens.* **2013**, 175428.
[20] Z. Li, A. V. Ferguson, *Neuroscience* **1993**, *55*, 197 – 207.

Received: April 27, 2016
Published online: July 12, 2016

